Article

Polystyrene as graphene film and 3D graphene sponge precursor

Alejandra Rendón-Patiño[1], Jinan Niu[1], Antonio Doménech-Carbó[2], Hermenegildo García[1,*] and Ana Primo[1,*]

[1] Instituto de Tecnología Química, Consejo Superior de Investigaciones Científicas-Universitat Politécnica de Valencia, Av. De los Naranjos s/n, 46022 Valencia, Spain.
[2] Departament de Química Analítica. Universitat de València. Dr. Moliner, 50, 46100 Burjassot (València) Spain.
* Correspondence: hgarcia@qim.upv.es; Tel.: +0034-963877807

Abstract: Polystyrene as a thin film on arbitrary substrates or pellets form defective graphene films or powders that can be dispersed in water and organic solvents. The materials were characterized by visible absorption, Raman and X-ray photoelectron spectroscopy, electron and atomic force microscopy and electrochemistry. Raman spectra of these materials show the presence of the expected 2D, G and D peaks at 2750, 1590 and 1350 cm^{-1}, respectively. The relative intensity of the G vs. the D peak is taken as a quantitative indicator of the density of defects in the G layer.

Keywords: graphene; polystyrene; 3D graphene sponges; electrochemistry

1. Introduction

Due to its wide availability and with the main objective of plastic wastes reutilization as carbon source, pyrolysis of polystyrene has attracted considerable attention.[1,2] Starting from the first report on 1950,[3-6] it was found that polystyrene decomposes in very high yields at temperatures above 370 °C affording a complex mixture of volatile compounds.[4-9] Polystyrene pyrolysis can be carried out at convenient rates at temperatures about 700 °C. Depending on temperature and operating conditions the formation in significant amounts in variable proportions of toluene, ethylbenzene, cumene, styrene and other benzene derivatives is observed.[8,10]

Since the target of all these studies has been the use of polystyrene wastes as feedstock,[1,11-13] the vast majority of the reports on polystyrene pyrolysis have focused on the analysis of the gas phase products, with the target being on the obtainment of a suitable mixture to be used as fuel. Surprisingly, as far as we know, none of these studies have paid attention to the nature of the possible solid residue that could remain after the pyrolysis. Evidence will be presented here showing that the residue of the polystyrene pyrolysis is a defective graphene.

A few years ago, we reported that pyrolysis of natural polysaccharides considered food and agricultural wastes is a suitable process for the preparation of defective graphenes either as a large area films on arbitrary substrates[14] or as a suspensions after sonication of the carbonaceous residue in liquid media.[15] About 40 % of the mass of these polymeric carbohydrates are converted into carbonaceous residue. On one hand, our contribution to this field was to show that these *filmogenic* polysaccharides form films on hydrophilic surfaces of appropriate substrates that upon pyrolysis are converted into continuous films of single or few-layers defective graphenes.[14] On the other hand, it was shown that pyrolysis of carbohydrate particles as powders and subsequent sonication of the carbonaceous residue renders dispersions of single or few-layers defective graphene particles in almost quantitative exfoliation yield.[15]

Although the procedure was adapted also to the preparation of doped and co-doped defective graphenes,[16-18] it has not been possible to decrease the oxygen content of the resulting graphenes

 doi:10.20944/preprints201811.0437.v1

below 10 wt%. The presence of residual oxygen is proposed to be due to the composition of the carbohydrates whose composition contains over 50 wt% in oxygen. After pyrolysis, a fraction of the initial oxygen content remains as oxygenated functional groups on the defective graphene sheet.

Continuing with alternative procedures for graphene preparation based on pyrolysis, either as films or as dispersible powders that could render graphene suspensions, it is of interest to explore the possibility to use also synthetic organic polymers that do not contain oxygen in its composition as precursors. In this way, it could be possible the formation of graphene materials lacking oxygen in their composition. In addition, a well-known property of synthetic plastic polymers is their ability to form high quality films on arbitrary supports what is a prerequisite to obtain graphene films.

Herein it will be shown that polystyrene, either cast as films on arbitrary surface or as pellets, upon pyrolysis at 900 °C form single or few layers graphenes or graphitic residues that can be efficiently dispersed as single or few layers graphene in liquid media. The procedure can be adapted to the formation of tridimensional (3D) graphene sponges by coating using silica spheres of uniform particle size as hard templates.

2. Materials and Methods

2.1 Preparation of Graphene films

Polystyrene (Mw 280,000 amu by GPC, Aldrich) was dissolved in dichloromethane at concentration of 3-30 mg/mL. The films were obtained by spin coating over 1x1 cm^2 quartz or Copper substrate (APT-POLOS spin-coater: 4000 rpm, 30 s). Polystyrene was pyrolysed under argon atmosphere using the following oven program: heating at 5 °C/min up to 900 °C for 2 h.

In an additional experiment, conversion of expanded polystyrene into graphene was performed by pyrolysis under argon atmosphere in a tubular oven heating at rate of 5 °C/min up to 900 °C for 2 h.

2.2 Preparation of graphene sponges

1 g of monodispersed silica spheres (80 nm) were suspended in a solution of polystyrene in dichloromethane at concentration of 50 mg/mL and stirred for 24 h under 40 °C reflux. This mixture was centrifuged at 4000 rpm for 5 min (Hettich Zentrifugen EBA 21) and washed twice with dichloromethane. After drying at 80 °C, the conversion of polystyrene into graphene was performed under argon atmosphere using an electrical furnace heating at rate of 2 °C/ min up to 900 °C for a holding time of 2 h. Then, the silica spheres were removed in a 2 M NaOH solution by stirring for 2 h at 80 °C. Finally, the product was collected by filtration.

2.3 Electrocatalytic measurements

Cyclic voltammetric (CV) and electrochemical impedance spectroscopy (EIS) measurements were performed at graphene sheets deposited onto glassy carbon electrode (geometrical surface area 0.071 cm^2) in a conventional three-electrode electrochemical cell completed with an Ag/AgCl (3 M NaCl) reference electrode and a Pt wire auxiliary electrode using a CH 660I potentiostat. Air-saturated 0.10 M potassium phosphate buffer solution at pH=7 was used as a supporting electrolyte incorporating 0.5 mM $K_3Fe(CN)_6$ plus 0.5 mM $K_4Fe(CN)_6$ as a redox probe. EIS experiments were performed upon application of a sinusoidal potential modulation of ±5 mV amplitude in the 10^5 Hz-10^{-1} Hz range. The bias potential was that of the equilibrium potential of the $Fe(CN)_6^{3-}/Fe(CN)_6^{4-}$ couple determined in CV measurements.

3. Results

3.1. Graphene films

Initial experiments were carried out by casting polystyrene (average MW 280 000) onto copper foils or rigid transparent quartz substrates. Figure 1 illustrates the procedure of the formation of defective graphene films. It has been reported that pyrolysis of polystyrene converts almost quantitatively this polymer into volatile organic compounds.[3] In agreement of these precedents, thermogravimetric analysis under inert atmosphere of our polystyrene sample indicates a weight loss about 99 %, confirming that most of the polymer has decomposed into volatile products.

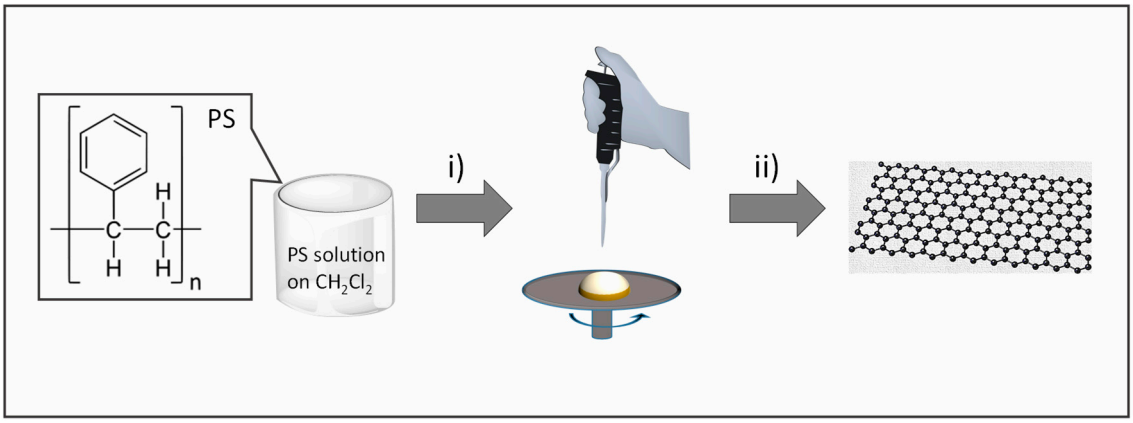

Figure 1. Illustration of the preparation procedure of defective graphene films by pyrolysis of polystyrene. i) spin coating of clean substrate with a CH_2Cl_2 solution of polystyrene; ii) pyrolysis under N_2 at 900 °C for 2 h.

In spite of an almost complete weight loss, and completing the previous studies analyzing volatile products, characterization of the substrate surface after the pyrolysis of polystyrene films shows the presence on these surfaces of defective graphene films, either as single layer, few-layers or multilayers. In accordance with the expected mass loss and also with the tendency of graphene layers to form stacks, the pyrolytic process results in a considerably decrease in the thickness of the resulting graphene films after pyrolysis that is about three orders of magnitude decrease of the initial polystyrene film thickness. In this way, micrometric polystyrene films typically result as a rule of thumb after the pyrolysis at 900 °C for 4 h under inert atmosphere into nanometric thick films corresponding to the stack of graphene layers. As an example, Figure 2 shows AFM images of a polystyrene film precursor that is converted in the pyrolysis into a defective few-layers graphene film.

Preprints (www.preprints.org) | NOT PEER-REVIEWED | Posted: 19 November 2018 doi:10.20944/preprints201811.0437.v1

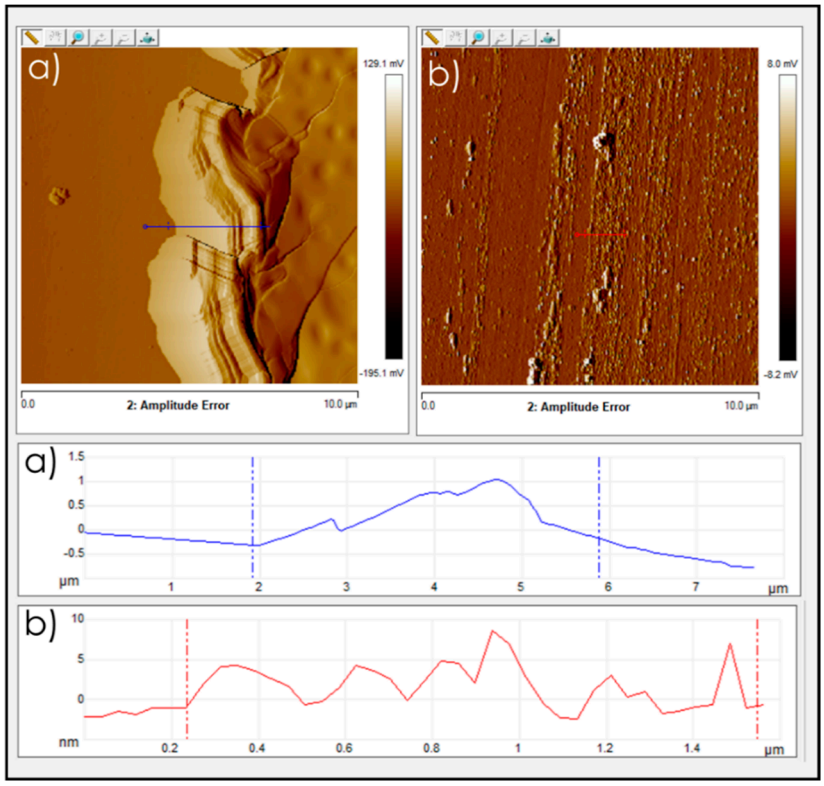

Figure 2. AFM images of a) polystyrene film precursor with a measured thickness of 1.5 µm and b) defective graphene film from pyrolysed polystyrene with a measured thickness of 5nm.

After the pyrolysis, the films were also characterized by Raman and visible absorption spectroscopy. The Raman spectra of the graphene films show the expected G band at about 1590 cm^{-1} accompanied by a D peak at 1350 cm^{-1} that is associated to the presence of defects on graphene. The presence of a 2D peak at 2700 cm^{-1} on top of a broad background was also observed. Figure 3c shows a representative example of the Raman spectra obtained for these defective graphene films. The relative intensity of the G vs. the D peak is usually taken as a quantitative indicator of the density of defects in the G layer.[19,20] In the present case the I_G/I_D ratio is about 1.19 that compares favorably with previous I_G/I_D ratio values reported in the literature, for instance for reduced graphene oxides that are about 0.9 [21] or even for defective graphenes obtained by pyrolysis of natural polysaccharides (I_G/I_D 1.15).[15]

Preprints (www.preprints.org) | NOT PEER-REVIEWED | Posted: 19 November 2018 doi:10.20944/preprints201811.0437.v1

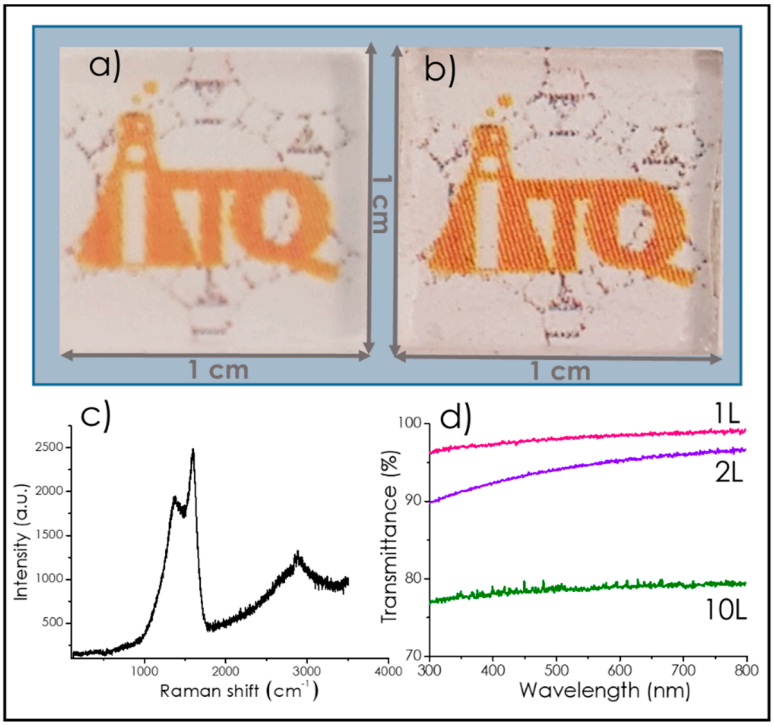

Figure 3. Photograph of quartz support with a) PS film before pyrolysis and b) graphene film after pyrolysis of PS; c) Raman spectrum recorded upon 514 nm excitation for defective graphene films on quartz obtained by pyrolysis of polystyrene films; d) Optical transmittance vs wavelength for 1 layer graphene film ([PS]= 3 mg/mL), 2 layers graphene film ([PS]= 10 mg/mL), 10 layers graphene film ([PS]= 30 mg/mL), spin coating rate 4,000 rpm.

For those films on quartz, optical transparency was in agreement with the number of layers of the resulting graphene films. As reported,[14,22,23] the optical transmittance measured at long wavelengths (660 nm) can serve to determine the number of layers of the samples. As an example, Figure 3 shows photographs of the polystyrene film on quartz before and the resulting defective few-layers graphene film after pyrolysis, as well as the relative transmittance of the samples.

The nature of the carbon atoms in the defective graphene film was determined by deconvolution of the C1s peak in high resolution XPS (Figure 4). Survey XPS analysis shows in the film the presence of C and O as the only detectable elements. Deconvolution of the C1s for films of defective graphene films on quartz substrates indicates that about 92 % of the carbon atoms are graphitic carbons appearing at the expected 284.5 eV binding energy.[24] It was estimated that about 8 % are sp^2 C atoms bonded to oxygen with a binding energy value of 286 eV. It should be commented that, depending on the nature of the substrate, the percentage of C atoms bonded to oxygen can increase respect to this value. In this way, using copper foils as substrates, the defective graphene films exhibit very similar Raman spectra as those presented in Figure 3, but in XPS the C1s peak was broader, more asymmetric, shifted towards higher binding energies and presented a significant larger contribution of C atoms bonded to O at 286.5 eV and even the presence of carboxylic C atoms in 6.4 % at 289.0 eV. Since the oxygen content of polystyrene precursor is negligible and the pyrolysis is carried out under inert atmosphere, XPS data suggests that the surface of the substrate is providing during the pyrolytic process some oxygen to the nascent defective graphene that becomes incorporated into the defective graphene. It should be remarked that no special precautions on the presence of surface oxides were taken in the case of copper foils. It also appears that quartz appears more reluctant than copper to act as oxygen donor during the pyrolysis. This seems to be in accordance with the chemical nature of copper that is more reducible in comparison with silicon.

Preprints (www.preprints.org) | NOT PEER-REVIEWED | Posted: 19 November 2018 doi:10.20944/preprints201811.0437.v1

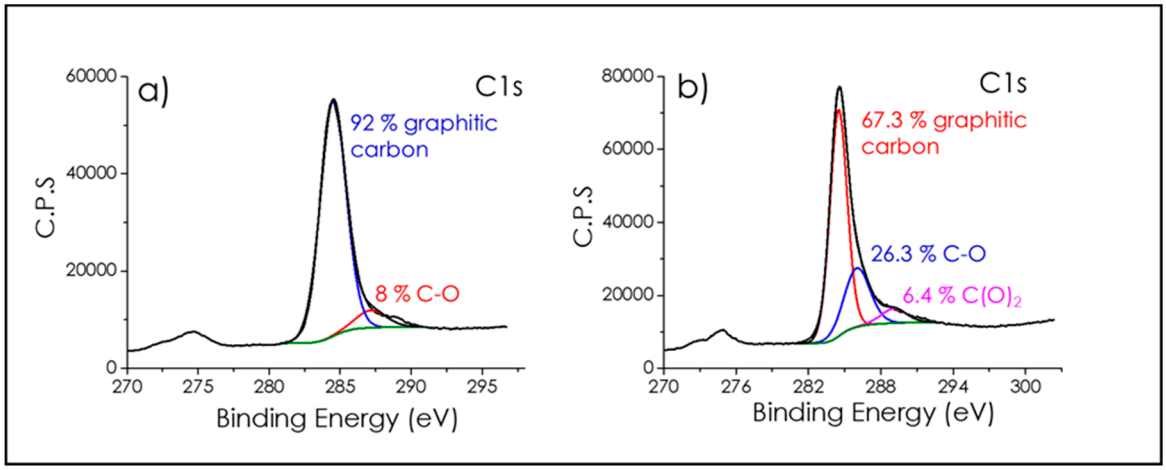

Figure 4. Deconvolution of the C1s peak in high resolution XPS of a) defective graphene on quartz support and b) defective graphene in Copper foil.

Scanning electron microscopy images of the defective graphene films after pyrolysis show a smooth continuous films at the submillimetric length scale (Figure 5a). Upon detaching some material from these films, transmission electron microscopy (TEM) images of the detached film can be taken. These images from the detached films show the expected layered morphology of the material. High resolution TEM images clearly show the structural ordering at the nanometric scale characteristic of graphene (Figure 5).

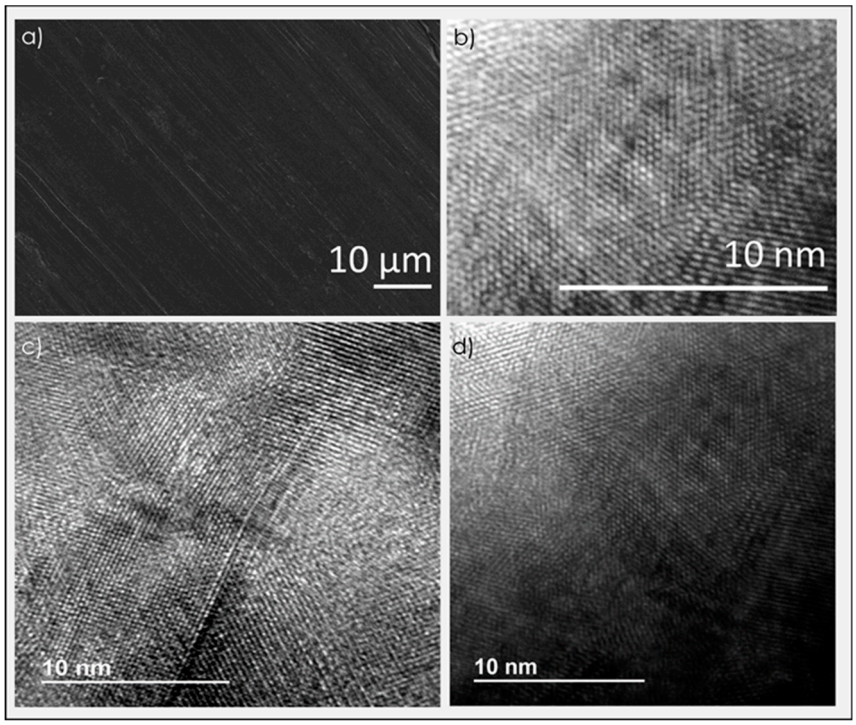

Figure 5. a) SEM images and b) high resolution TEM images of the defective graphene films after pyrolysis and c) and d) High resolution TEM images of defective graphene from polystyrene pellets.

Films on quartz of defective few-layers graphene obtained from polystyrene exhibit a notable electrical conductivity in the range below kΩ/square, typically about 170 and 270 Ω/square. This electrical conductivity was sufficiently high to allow recording high resolution scan tunneling

 doi:10.20944/preprints201811.0437.v1

microscopy (STM) of the samples. Figure S1 (supporting information) presents an illustrative example of the images taken for these defective graphene films, showing the presence of atoms in the expected arrangement. Unfortunately, the lack of sufficient flatness of the quartz substrate, particularly after being submitted to the thermal stress of the pyrolysis process, precludes recording the image of a large area of these films. It should be noted in this context that previous attempts to record STM images of defective graphene films from chitosan and alginate pyrolysis met with failure, due to their insufficient electrical conductivity. In this regard, the behavior of polystyrene derived graphene films are remarkable compared to precedents in the literature that report STM for high quality graphene films prepared by chemical vapor deposition on facet oriented clean metal surface.[25]

Besides films, polystyrene was also pyrolyzed as pellets. It was observed that during the initial stages of temperature increase, polystyrene pellets melt and coat the ceramic crucible used in the pyrolysis process forming a spontaneously a high quality film. If the amount of polystyrene in the crucible is large, films of several millimeters thickness can be obtained due to melting of the plastic. At the end of the pyrolysis, bright metallic carbon residues coating the ceramic crucible are formed. For thick films, the carbonaceous residue can be recovered from the crucible by scratching and the solid suspended by sonication on various solvents. Figure 5 also provides some TEM images of the graphene material present in the suspensions, whereby the typical hexagonal atomic arrangement characteristic of graphene can also be observed.

The films of defective graphenes on glassy carbon electrodes were characterized electrochemically by electrochemical impedance spectroscopy (EIS) and cyclic voltammetry (CV) using $Fe(CN)_6^{3-}/Fe(CN)_6^{4-}$ couple as a redox probe. EIS of defective graphene films is shown in Figure 6. The experimental data were satisfactorily modeled using the Randles-type equivalent circuit (see inset in Figure 6) composed by solution resistance (R_s) in series with a parallel combination of a constant phase element (Q_{dl}) representative of the non-ideal capacitance at the electrolyte/sheet interface with a branch containing a resistance (R_{ct}), representative of the charge-transfer resistance at the above interface, in series with a Warburg element (W), representative of the existing diffusive effects. This equivalent circuit is coincident with that proposed for describing the EIS of graphene oxide sheets on glassy carbon electrode.[26-28] The R_s, R_{ct}, Q_{dl} and W values determined from the EIS of these defective graphene films were 200 Ω, 7900 Ω, 6.8×10^{-5} Ω s^{-n} (n 0.92) and 2.3×10^{-3} Ω$\times s^{-1/2}$, respectively.

Cyclic voltammograms of the $Fe(CN)_6^{3-}/Fe(CN)_6^{4-}$ redox pair at the defective graphene film on glassy carbon displayed the characteristic peaks for the essentially reversible interconversion of the two species (Figure 6). The peak current corresponds to an effective electrochemical area of the working graphene electrodes 4.8 times larger than the geometrical surface area of the bare glassy carbon electrode.

Preprints (www.preprints.org) | NOT PEER-REVIEWED | Posted: 19 November 2018 doi:10.20944/preprints201811.0437.v1

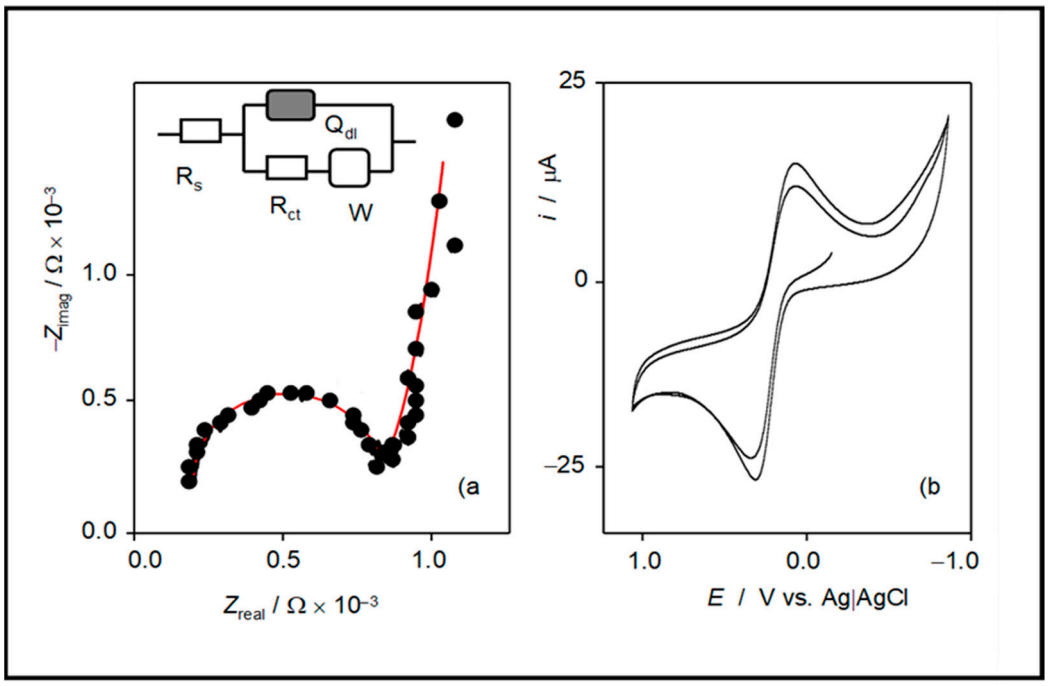

Figure 6. Electrochemical characterization of graphene films deposited on glassy carbon electrode in contact with 1.0 mM $K_3Fe(CN)_6/K_4Fe(CN)_6$ solution in 0.10 M potassium phosphate aqueous solution at pH 7.0. a) Nyquist plot of EIS at a bias potential of 0.20 V vs. Ag/AgCl; b) CV, potential scan rate 20 mV/s. The inset in Fig. 6a corresponds to the equivalent circuit providing the theoretical impedance spectrum depicted as the continuous line in the same.

3.2. 3D graphene sponges

Besides forming flat films, the possibility to exploit the filmogenic ability of polystyrene to adopt the form of the substrates for the formation of 3D graphene sponges was considered. Structuring of graphene into 3D objects is important as a way to increase the surface area of the material, for instance in the preparation of electrodes and supercapacitors, among other possible applications.[29-32] A general strategy to obtain 3D graphene sponges with regular pore size is the use of hard templates.[33] Silica spheres of uniform diameter are among the preferred hard templates to form 3D sponges.[34] In some procedures, graphene was formed by chemical vapor deposition on the silica spheres as templates[35] or graphene oxide was adhered to the silica spheres and used as precursor of reduced graphene oxide sponges.[33]

In the present study, silica spheres of uniform dimensions about 80 nm were prepared by the Stöber hydrolysis procedure and used as templates.[36] These silica spheres were impregnated with polystyrene by stirring a suspension of both components in CH_2Cl_2. After recovery of the impregnated spheres and washings to remove polystyrene excess, pyrolysis of the impregnated silica spheres was carried out at 900 °C under N_2 atmosphere. The silica spheres were removed by etching of the resulting carbonaceous composite material with NaOH. Figure 7 summarizes the procedure for the preparation of the 3D defective graphene sponges.

Preprints (www.preprints.org) | NOT PEER-REVIEWED | Posted: 19 November 2018 doi:10.20944/preprints201811.0437.v1

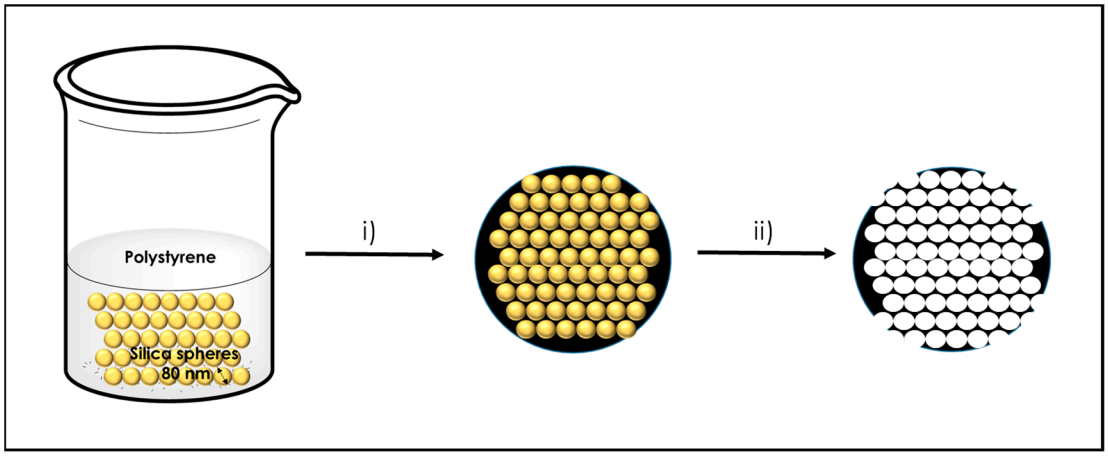

Figure 7. Illustration of the preparation procedure of 3D defective graphene sponges.

Raman and X-ray photoelectron spectroscopy of the 3D defective graphene sponges were mostly coincident with those previously commented. Interestingly, SEM images of the 3D porous graphene sponge after removal of the silica spheres shows the presence of a regular porosity in the material. Figure 8 shows some selected images at different magnifications to illustrate the morphological features of the 3D graphene sponges prepared from polystyrene.

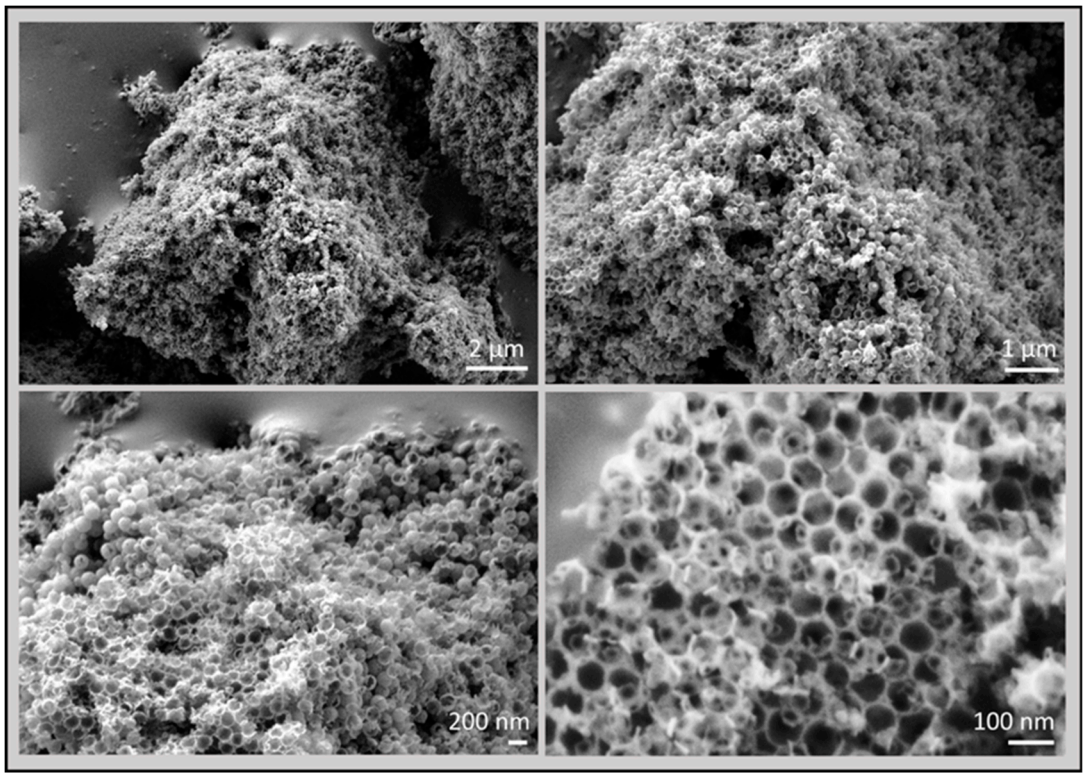

Figure 8. SEM images at different magnifications of 3D graphene sponges prepared from polystyrene.

As observed in these images, the 3D graphene sponge morphology is constituted by hexagonal cavities of very uniform dimensions of about 80 nm. This dimension is commensurate with the diameters of the silica spheres used as templates. These cages have four windows of about 40 nm diameter that are tetrahedrally arranged. The thickness of the wall is about 5 nm that is consistent with them being constituted by few-layers defective graphene.

4. Conclusions

Although pyrolysis of graphene has been exhaustively studied as a way to convert this synthetic polymer into fuels, no attention was paid to the possibility to form graphene. In the present manuscript, it has been shown that pyrolysis of polystyrene films or pellets form defective graphenes either as films or as residues that can be dispersed in liquid media. Depending on the nature of the substrate, the resulting graphene can incorporate oxygen in a variable percentage. The notable electrical conductivity of these defective graphene films allows to monitor the surface by scanning tunneling microscopy and to use these films as electrodes. The filmogenic properties of polystyrene make also possible the preparation of 3D graphene sponges with remarkable uniform pore size by using silica spheres as hard templates. The present finding paves the way to the preparation of doped defective graphene and heterojunctions by taken advantage of the ability of polystyrene to form these graphenes.

Supplementary Materials: The following are available online, Figure S1: High resolution scan tunneling microscopy (STM) of defective graphene using polystyrene as precursor.

Author Contributions: The research has been performed with the contribution of all the authors. The concept of the study was developed by J.N., A.P. sand H.G. Sample preparation and characterization was performed by A.R.-P. and J.N. Electrochemical measurements were carried out by A.D. Drafting of the manuscript was performed by H.G. and A.P. All the authors correct and read the manuscript.

Funding: This research was funded by the Spanish Ministry of Economy and Competitiveness (Severo Ochoa and CTQ2015-68653-CO2-R1) and Generalitat Valenciana (Prometeo 2017-083).

Acknowledgments: AP thanks the Spanish Ministry for a Ramón y Cajal research associate contract.

Conflicts of Interest: The authors declare no conflict of interest.

References

1. Scheirs, J.; Kaminsky, W. *Feedstock recycling and pyrolysis of waste plastics*; John Wiley & Sons Chichester, UK: 2006.
2. Kaminsky, W. Chemical recycling of mixed plastics of pyrolysis. *Advances in Polymer Technology: Journal of the Polymer Processing Institute* **1995**, *14*, 337-344.
3. E., A. Pyrolysis of polystyrene. *Journal of Polymer Science* **1950**, *5*, 378-379, doi:doi:10.1002/pol.1950.120050310.
4. Karaduman, A.; Şimşek, E.; Cicek, B.; Bilgesü, A. Flash pyrolysis of polystyrene wastes in a free-fall reactor under vacuum. *Journal of Analytical and Applied Pyrolysis* **2001**, *60*, 179-186.
5. Kim, S.-S.; Kim, S. Pyrolysis characteristics of polystyrene and polypropylene in a stirred batch reactor. *Chemical Engineering Journal* **2004**, *98*, 53-60.
6. Liu, Y.; Qian, J.; Wang, J. Pyrolysis of polystyrene waste in a fluidized-bed reactor to obtain styrene monomer and gasoline fraction. *Fuel Processing Technology* **2000**, *63*, 45-55, doi:https://doi.org/10.1016/S0378-3820(99)00066-1.

7. Bradt, P.; Dibeler, V.H.; Mohler, F.L. A new technique for the mass spectrometric study of the pyrolysis products of polystyrene. *Journal of Research of the National Bureau of Standards* **1953**, *50*, 201-202.
8. Cameron, G. Mechanism of volatile production during pyrolysis of polystyrene. *Die Makromolekulare Chemie: Macromolecular Chemistry and Physics* **1967**, *100*, 255-261.
9. Hussain, Z.; Khan, K.M.; Perveen, S.; Hussain, K.; Voelter, W. The conversion of waste polystyrene into useful hydrocarbons by microwave-metal interaction pyrolysis. *Fuel processing technology* **2012**, *94*, 145-150.
10. Onwudili, J.A.; Insura, N.; Williams, P.T. Composition of products from the pyrolysis of polyethylene and polystyrene in a closed batch reactor: Effects of temperature and residence time. *Journal of Analytical and Applied Pyrolysis* **2009**, *86*, 293-303.
11. Kaminsky, W.; Predel, M.; Sadiki, A. Feedstock recycling of polymers by pyrolysis in a fluidised bed. *Polymer Degradation and Stability* **2004**, *85*, 1045-1050.
12. Angyal, A.; Miskolczi, N.; Bartha, L. Petrochemical feedstock by thermal cracking of plastic waste. *Journal of analytical and applied pyrolysis* **2007**, *79*, 409-414.
13. Miandad, R.; Nizami, A.; Rehan, M.; Barakat, M.; Khan, M.; Mustafa, A.; Ismail, I.; Murphy, J. Influence of temperature and reaction time on the conversion of polystyrene waste to pyrolysis liquid oil. *Waste management* **2016**, *58*, 250-259.
14. Primo, A.; Atienzar, P.; Sanchez, E.; Delgado, J.M.; García, H. From biomass wastes to large-area, high-quality, N-doped graphene: catalyst-free carbonization of chitosan coatings on arbitrary substrates. *Chemical communications* **2012**, *48*, 9254-9256.
15. Primo, A.; Sánchez, E.; Delgado, J.M.; García, H. High-yield production of N-doped graphitic platelets by aqueous exfoliation of pyrolyzed chitosan. *Carbon* **2014**, *68*, 777-783.
16. Latorre-Sánchez, M.; Primo, A.; García, H. P-Doped Graphene Obtained by Pyrolysis of Modified Alginate as a Photocatalyst for Hydrogen Generation from Water–Methanol Mixtures. *Angewandte Chemie International Edition* **2013**, *52*, 11813-11816.
17. Dhakshinamoorthy, A.; Primo, A.; Concepcion, P.; Alvaro, M.; Garcia, H. Doped Graphene as a Metal-Free Carbocatalyst for the Selective Aerobic Oxidation of Benzylic Hydrocarbons, Cyclooctane and Styrene. *Chemistry–A European Journal* **2013**, *19*, 7547-7554.
18. Dhakshinamoorthy, A.; Latorre-Sanchez, M.; Asiri, A.M.; Primo, A.; Garcia, H. Sulphur-doped graphene as metal-free carbocatalysts for the solventless aerobic oxidation of styrenes. *Catalysis Communications* **2015**, *65*, 10-13.
19. Cançado, L.G.; Jorio, A.; Ferreira, E.M.; Stavale, F.; Achete, C.; Capaz, R.; Moutinho, M.; Lombardo, A.; Kulmala, T.; Ferrari, A. Quantifying defects in graphene via Raman spectroscopy at different excitation energies. *Nano letters* **2011**, *11*, 3190-3196.
20. Eigler, S.; Dotzer, C.; Hirsch, A. Visualization of defect densities in reduced graphene oxide. *Carbon* **2012**, *50*, 3666-3673.
21. Stankovich, S.; Dikin, D.A.; Piner, R.D.; Kohlhaas, K.A.; Kleinhammes, A.; Jia, Y.; Wu, Y.; Nguyen, S.T.; Ruoff, R.S. Synthesis of graphene-based nanosheets via chemical reduction of exfoliated graphite oxide. *carbon* **2007**, *45*, 1558-1565.
22. Reina, A.; Jia, X.; Ho, J.; Nezich, D.; Son, H.; Bulovic, V.; Dresselhaus, M.S.; Kong, J. Large area, few-layer graphene films on arbitrary substrates by chemical vapor deposition. *Nano letters* **2008**, *9*, 30-35.
23. Wassei, J.K.; Kaner, R.B. Graphene, a promising transparent conductor. *Materials today* **2010**, *13*, 52-59.

24. Panchakarla, L.; Subrahmanyam, K.; Saha, S.; Govindaraj, A.; Krishnamurthy, H.; Waghmare, U.; Rao, C. Synthesis, structure, and properties of boron-and nitrogen-doped graphene. *Advanced Materials* **2009**, *21*, 4726-4730.
25. Varykhalov, A.; Sánchez-Barriga, J.; Shikin, A.; Biswas, C.; Vescovo, E.; Rybkin, A.; Marchenko, D.; Rader, O. Electronic and magnetic properties of quasifreestanding graphene on Ni. *Physical review letters* **2008**, *101*, 157601.
26. Casero, E.; Parra-Alfambra, A.; Petit-Domínguez, M.; Pariente, F.; Lorenzo, E.; Alonso, C. Differentiation between graphene oxide and reduced graphene by electrochemical impedance spectroscopy (EIS). *Electrochemistry Communications* **2012**, *20*, 63-66.
27. Bonanni, A.; Pumera, M. High-resolution impedance spectroscopy for graphene characterization. *Electrochemistry Communications* **2013**, *26*, 52-54.
28. Song, Y.; Feng, M.; Zhan, H. Geometry-dependent electrochemistry of graphene oxide family. *Electrochemistry Communications* **2015**, *56*, 38-42.
29. Zhang, L.; Zhang, F.; Yang, X.; Long, G.; Wu, Y.; Zhang, T.; Leng, K.; Huang, Y.; Ma, Y.; Yu, A. Porous 3D graphene-based bulk materials with exceptional high surface area and excellent conductivity for supercapacitors. *Scientific reports* **2013**, *3*, 1408.
30. Zhao, J.; Ren, W.; Cheng, H.-M. Graphene sponge for efficient and repeatable adsorption and desorption of water contaminations. *Journal of Materials Chemistry* **2012**, *22*, 20197-20202.
31. Gao, H.; Duan, H. 2D and 3D graphene materials: Preparation and bioelectrochemical applications. *Biosensors and Bioelectronics* **2015**, *65*, 404-419.
32. Zhou, G.; Paek, E.; Hwang, G.S.; Manthiram, A. Long-life Li/polysulphide batteries with high sulphur loading enabled by lightweight three-dimensional nitrogen/sulphur-codoped graphene sponge. *Nature communications* **2015**, *6*, 7760.
33. Han, S.; Wu, D.; Li, S.; Zhang, F.; Feng, X. Porous graphene materials for advanced electrochemical energy storage and conversion devices. *Advanced materials* **2014**, *26*, 849-864.
34. Huang, X.; Qian, K.; Yang, J.; Zhang, J.; Li, L.; Yu, C.; Zhao, D. Functional nanoporous graphene foams with controlled pore sizes. *Advanced Materials* **2012**, *24*, 4419-4423.
35. Xia, X.; Chao, D.; Zhang, Y.Q.; Shen, Z.X.; Fan, H.J. Three-dimensional graphene and their integrated electrodes. *Nano Today* **2014**, *9*, 785-807.
36. Stöber, W.; Fink, A.; Bohn, E. Controlled growth of monodisperse silica spheres in the micron size range. *Journal of colloid and interface science* **1968**, *26*, 62-69.